Supplemental Material

February 21, 2018

Further selection and observational details are presented here. We report the photometric qualities that led to J1100-0053 being targeted and the specifics of the repeat spectroscopy. We also discuss alternative scenarios that could explain the observations, and why we dismiss these in turn, while giving further details of our preferred model.

1 Further Observational Details

1.1 Optical Imaging

SDSS J110057.70-005304.5 was first detected in the National Geographic Society-Palomar Observatory Sky Survey [NGS-POSS; 1, 30] in 1955 April. It is catalogued in the SuperCOSMOS Science Archive [SSA; 17, 18] and due to its equatorial position was also observed by the UK Schmidt Telescope [UKST; 11, 12]. Querying the SSA returns *gCorMag* and *sCorMag* which are the magnitudes assuming the object is either a galaxy or star, respectively. We use the *sCorMag* values as is appropriate for an image with flux dominated by the point-like AGN; the *sCorMag* magnitudes are calibrated in the Vega system. For J1100-0053 we find the magnitudes are: 18.10 mag in the blue UK-J filter from MJD 45440.47 (1983 April 16); 17.49 mag in the red POSS-I 'E'-filter from MJD 35214.22 (1955 April 17); 17.92 mag in the red UK-R filter from MJD 46521.47 (1986 April 01) and 17.71 mag in the UK-I filter from MJD 47273.49 (1988 April 22). J1100-0053 is not in the Digital Access to a Sky Century @ Harvard (DASCH[1]).

J1100-0053 was observed by Röntgensatellit (ROSAT) and appears in the All-Sky Survey Bright Source Catalogue [RASS-BSC; 7, 46]. J1100-0053 was imaged by the Sloan Digital Sky Survey (SDSS) in the *u*, *g*, *r*, *i* and *z*-bands and satisfied a number of spectroscopic targeting flags making it a quasar target [37]. J1100-0053 is in Data Release 3 (DR3) of the Dark Energy Camera Legacy Survey (DECaLS), where there are 8, 3 and 9 exposures in the *g*, *r* and *z*-band respectively. The *g*- and *r*-band observations span roughly a year, ($56707 \leq g_{\rm MJD} \leq 56727$ and $56367 \leq r_{\rm MJD} \leq 56367$), while the *z*-band observations span almost 3 years ($56383 \leq z_{\rm MJD} \leq 57398$).

1.2 SDSS and BOSS Spectroscopy

A spectrum was obtained on MJD 51908 (SDSS Plate 277, Fiber 212) and the spectrum of a $z = 0.378$ quasar was catalogued in the SDSS Early Data Release [39, 44]. The physical properties of J1100-0053 derived from the MJD 51908 spectrum using the methods in Shen et al. [41], are given in Table 1, where we also give the properties of J2314+0005 [16] and J1052+1519 [43] for comparison.

The second epoch spectrum is from the SDSS-III Baryon Oscillation Spectroscopic Survey [BOSS; 13] and shows the downturn at $\lesssim$4300Å. SDSS-III BOSS actively vetoed known $z < 2$ QSOs [38], but due to J1100-0053 being selected as an ancillary target [via a white dwarf program; 20, 21] a second spectral epoch was obtained. Due to a design tradeoff to improve throughput in the Lyα-forest of quasar spectra in BOSS, QSO targets were subject to spectrophotometric calibration errors [25]. These are introduced primarily due to offsets in fiber-hole positioning between quasar targets and spectrophotometric standard stars. However, since J1100-0053 was *not* a BOSS QSO *target*, it is not subject to this "blue offset". J1100-0053 has no pipeline flag suggesting the spectrum was compromised during data taking. We

[1] http://dasch.rc.fas.harvard.edu/project.php

Quantity	this paper	Guo et al. (2016)	Stern et al. (2018)
SDSS name	J110057.70-005304.5	J231742.60+000535.1	J105203.55+151929.5
R.A. / deg	165.240463	349.42752075	163.01480103
Declination / deg	-0.884586	+0.093091	15.32488632
redshift, z	0.3778±0.0003	0.3209±0.0002	0.3022±0.0008
SDSS Plate, Fiber, MJD	277, 212, 51908(*)	382, 173, 51816(*) 679, 551, 52177 680, 346, 52200	2483, 204, 53852(*)
BOSS Plate, Fiber, MJD	3836, 258, 55302	–	–
$M_i(z=2)$ / mag	-24.48	-23.65	-22.73
log $(L_{\rm bol}/{\rm ergs}^{-1})$	45.78±0.02	45.56±0.004	45.07±0.004
log $(M_{\rm BH}/M_{\odot})$	8.83±0.14	8.43±0.03	8.46±0.02
Eddington ratio (%)	7.0	10.7	3.2

Table 1: Physical properties of J1100-0053, J2317+0005 and J1052+1519 using the methods from Shen et al. [41]. (*)This spectrum was used to estimate the quantities reported.

checked the calibration of BOSS Plate 3836 that observed J1100-0053 and confirmed that the data were high-SNR and that the behaviour in the blue spectrum was not due to the instrument, telescope or data reduction.

1.2.1 Palomar Spectroscopy

A third epoch spectrum was obtained from the Palomar Hale 5m telescope using the Double Spectrograph (DBSP) instrument. Exposures of 600s and 300s were taken in good conditions on 2017 February 25 (MJD 57809). Features to note include the continuum straddling Mg II being blue in the 2017 spectrum, as it was for the SDSS spectrum in 2000, as opposed to red, as it was for the BOSS spectrum in 2010. A fourth spectral epoch was also taken using the Hale 5m and DBSP on 2018 January 14 (MJD 58132). There has been very little, if any change seen since the third spectral epoch.

1.3 Selection in NEOWISE-R of J1100-0053

We use data from the beginning of the WISE mission [2010 January; 47] through the first-year of NEOWISE-R operations [2014 December; 24]. The WISE scan pattern leads to coverage of the full-sky approximately once every six months, but the satellite was placed in hibernation in 2011 February and then reactivated in 2013 October. Hence, our light curves have a cadence of 6 months with a 32 month sampling gap.

The W1/W2 light curves for ∼200,000 SDSS and BOSS spectroscopic quasars are obtained by performing forced photometry at the locations of DECam-detected optical sources [23, 28, 29]. This forced photometry is performed on time-resolved coadds [23], each of which represents a stack of ∼12 exposures. As noted above, a given sky location is observed by WISE for ∼1 day once every six months, which means that the forced photometry light curves typically have four coadd "epochs" available. Coadd epochs of a given object are separated by a minimum of six months and a maximum of four years. The coaddition removes the possibility of probing variability on $\lesssim$1 day time scales, but pushes ≈1.4 magnitudes deeper than individual exposures while removing virtually all single-exposure artifacts (e.g. cosmic rays and satellites).

Approximately ∼30,000 of the SDSS/BOSS quasars with W1/W2 light-curves available are "IR-bright", in that they are above both the W1 and W2 single exposure thresholds and therefore detected at very high significance in the coadds. For this ensemble of objects, the typical variation in each quasar's measured (W1-W2) color is 0.06 magnitudes. This includes statistical and systematic errors which are expected to contribute variations at the few hundredths of a magnitude level. The typical measured single-band scatter is 0.07 magnitudes in each of W1 and W2.

We undertook a search for outliers relative to these trends. Specifically, we selected objects with the following characteristics:

- Monotonic variation in both W1 and W2 flux.
- W1 flux and W2 flux Pearson correlation coefficient $r \geq 0.9$.
- > 0.5 mag peak-to-peak variation in either W1 or W2.

This yields a sample of 248 sources. 31 of these are assumed to be blazars due to the presence of Faint Images of the Radio Sky at Twenty-Centimeters [FIRST; 9] radio counterparts, and we discount them for further analyses. Another 22 objects are outside the FIRST footprint, leaving 195 quasars in our IR-variable sample.

1.4 Additional Multiwavelength data for J1100-0053

J1100-0053 is detected in ROSAT as 2RXS J110058.1-005259 with 27.00 counts (count error 6.14) and a count rate = 0.06±0.01 counts s^{-1} [10]. The NASA/IPAC Extragalactic Database (NED[2]) gives J1100-0053 as $1.27 \pm 0.28 \times^{-12}$ erg cm^{-2} s^{-1} in the 0.1-2.4 keV range (unabsorbed flux). J1100-0053 is not in either the *Chandra* or *XMM-Newton* archives but is detected by the Galaxy Evolution Explorer [GALEX; 26, 31] and has reported 19.29 ± 0.12 mag in the far-UV and 18.89 ± 0.05 mag in the near-UV. As noted above, there is no source within 30 arcsec in the FIRST survey, i.e. at 21cm radio frequencies. None of the *Hubble Space Telescope*, the *Spitzer Space Telescope* or the *Kepler* missions have observed J1100-0053. It is also not in the Hyper Suprime-Cam (HSC) Data Release 1 [6] footprint.

2 Further Model Details

In a similar vein to the discussion in [43], in this section we discuss several models with the aim of determining the physical mechamism(s) driving the light curve and spectral behaviour of J1100-0053. The explanations come in two broad classes: obscuration and changes in the accretion disk. Ultimately, we are forced towards a model of the latter type that combines a cooling front propagating in the accretion disk along with changes in the disk opacity.

Scenario I: Obscuring by an Infalling Cloud

We explore the possibility that an obscuring cloud, or clouds, cause the observed light curve and spectral behaviour of J1100-0053. In this scenario, the obscuring cloud(s) are required to cross the line of sight. The cloud(s) also need to block most of the inner disk such that the ionizing radiation could not impact on the BLR or the torus for a period of months-years, in order to explain both the IR drop and broadline disappearance. An explanation of why the light curves 'recover' after a period of ~ 2500 days (observed-frame) is also required; i.e., why do the light curves not rapidly return to their original flux levels once the obscuring event is over.

Clouds should not typically infall; they need to lose angular momentum if they are drawn from a distribution with Keplerian orbits, and even if they do lose angular momentum, e.g., in a collision with approximately equal mass, they would likely be either destroyed or no longer coherent. The relevant timescales here are the freefall and cloud-crushing times. The freefall timescales are:

$$t_{\rm ff} \sim 100{\rm yr} \left(\frac{\rm r}{0.4{\rm pc}} \right)^{3/2} \left(\frac{\rm M}{10^8 {\rm M}_\odot} \right)^{-1} \quad (1)$$

[2]https://ned.ipac.caltech.edu/

and Kelvin-Helmholtz instabilities would destroy the clouds within the cloud-crushing time, [e.g., 8, 19, 32, 42], given by

$$t_{\rm cc} \sim 100{\rm yr}\left(\frac{\rho_{\rm cloud}/\rho_{\rm medium}}{10^6}\right)^{1/2}\left(\frac{\rm r_{cloud}}{4\times10^{10}{\rm km}}\right)\left(\frac{\rm v_{rel}}{10^4{\rm km/s}}\right)^{-1}. \quad (2)$$

Thus, even if clouds did infall, they would end up fragmented, which should pollute the inner disk. The dust in the cloud would then be well inside the dust sublimation radius:

$$R_{\rm dust} \approx 0.4{\rm pc}\left(\frac{\rm L}{10^{45}{\rm erg/s}}\right)^{1/2}\left(\frac{\rm T_{sub}}{1500{\rm K}}\right)^{2.6} \quad (3)$$

and so the dust will be destroyed in the ∼100 year free-fall from the dust-sublimation region. Hence, one can not absorb the UV spectrum with dust, since it will have been sublimated well before it arrives at the inner disk.

Scenario II: Accretion Disk model

Having discounted an obscuring event as the explanation for J1100-0053, we turn to accretion disk models [see also the recent review by 48]. We describe as 'cold' accretion flows that are optically thick, geometrically thin and which drive relatively high mass accretion rates. They are 'cold' in the sense that the virial temperature of particles near the black hole is low. Similarly, we characterize optically thin, geometrically thick and low mass accretion rate flows as virially 'hot' accretion flows.

After giving our model set-up, we discuss whether J1100-0053 can be described by a 'hot' accretion flow, such as the advection-dominated accretion flow. We then discuss our preferred 'cold' accretion flow model~~, but~~ where the temperature of the accretion disk is perturbed by propagating cooling and heating fronts in the inner parts ($\leq 1000r_g$) of the accretion disk. Our disk remains virially cold throughout this cycle.

2.1 Model set-up

We start with a multitemperature blackbody (MTB) model, with a $L \propto T^4$ dependence and a $T \propto r^{-3/4}$ relation. A thin accretion disk has a negligible radial pressure gradient. Therefore, at each radius R the gas orbits at the Keplerian angular frequency, $\Omega_{\rm K} = (GM/r^3)^{1/2}$, where M is the mass of the central object. An element possesses specific angular momentum $l = rv_\phi = r^2\Omega = \sqrt{GMr}$, and in a steady state, the loss of angular moment is $\dot{J} = \dot{M}l(r) = \dot{M}\sqrt{GMr_d}$. From [49] the zero torque (ZT) luminosity is given by:

$$L_{\rm disk} = \frac{GM\dot{M}}{2r_{\rm in}} = 73.9\sigma\left(\frac{T_{\rm max}}{f}\right)^4 r_{\rm in}^2 \quad (4)$$

and the standard, non-zero torque (NZT) luminosity is given by:

$$L_{\rm disk} = \frac{3GM\dot{M}}{2r_{\rm in}} = 12.6\sigma\left(\frac{T_{\rm max}}{f}\right)^4 r_{\rm in}^2 \quad (5)$$

The early 2000s spectrum is well fit with a thin, Shakura & Sunyaev [40] α-disk. The 2010 spectrum and the sharp fall-off at $\sim 200-300$nm, is not reproducible using a different temperature profile alone, even one where the entire inner disk (unphysically) vanishes. This is due to the width of the Planck function in wavelength space. For the same reasons, a gray absorber model with uniformly suppressed emission at small disk radii is also incapable of fitting our 2010 (or the J2317+0005 spectrum in [16]). Wavelength dependent absorption, combined with a lower disk emissivity is required.

Model 'A': Switching states to an RIAF/ADAF: A possible explanation for the behaviour of J1100-0053 is that it switches accretion modes, from a "cold", high $\dot{M}$ flow to a hotter, lower $\dot{M}$ flow, with the latter being i.e., a radiatively inefficient accretion flow [RIAF; see reviews by 34, 36] or an advection-dominated accretion flow [ADAF; 48, and references therein].

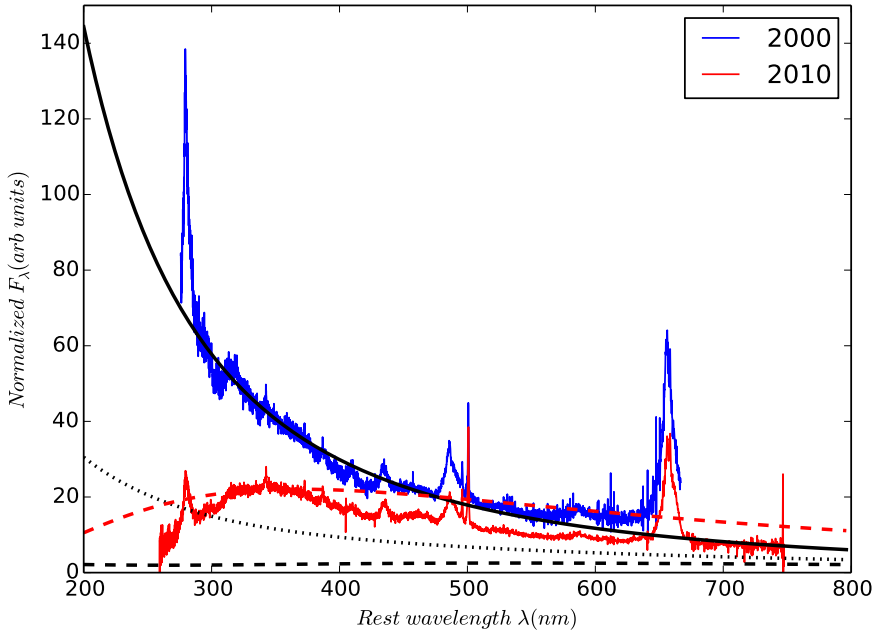

Figure 1: J1100-0053 data (blue line 2000 spectrum; red line 2010 spectrum) and 4 models. Solid black line shows non-zero torque at ISCO [following 4]; dotted and dashed black lines show temperature suppression inside $r_{\rm alt} = 225 r_{\rm g}$, such that the spectral flux is $f_{\rm dep} = 0.2$ or 0.01 (respectively) compared to a zero torque model; dashed red line shows zero flux inside $r_{\rm alt} = 80 r_{\rm g}$ and arbitrary normalization to match peak of 2010 spectrum. Note the poor fit due to the intrinsic width of the thermal peak.

There are examples of this type of behaviour in lower-luminosity objects. For example, Nemmen et al. [35] successfully explain the SED for the low-ionization nuclear emission-line region (LINER) of NGC 1097 with a model where the inner part of the flow is a (virially hot) RIAF, and the outer part as a standard (virially cold) thin disk.

The broadband spectrum of NGC 1097 from Nemmen et al. [35] initially appears similar to the UV/optical 2010 spectrum of J1100-0053. In Nemmen et al. [35, e.g., their Figure 4], there are disk model components that look similar to the fall-off at 200nm observed in the J1100-0053 2010 spectrum. This would involve a thin disk component extending from $\sim 450 r_g$ to the outer regions of the disk. Figure 4 in Nemmen et al. [35] shows the Multicolor Disk (MCD) blackbody-like model component from the thin disk at $r > 225 r_g$ (their long dashed line) dramatically decreasing at $\sim 10^{15}$Hz ($\sim$ 300nm). Nemmen et al. [35] model the disk region interior to this as a RIAF at a power (in νL_ν), an order of magnitude lower than the MCD in the optical, but spanning from the X-ray to the far-IR.[3]

Can J1100-0053 switch states from a thin disk quasar to an ADAF at small radii with the thin disk surviving at large radii? Assuming the transition happens due to an instability on the thermal timescale of the disk, then at large radii the thermal timescale is

$$t_{\rm th} \sim 14 \text{ years } \left(\frac{\alpha}{0.03}\right)^{-1} \left(\frac{r}{225 r_g}\right)^{3/2} \frac{r_g}{c} \tag{6}$$

and is too long given the observations. However, if the viscosity parameter α increases to $\alpha \approx 0.3$, as suggested by King et al. [22], then the thermal timescale is $t_{\rm th} \sim 1.4$ year and the front timescale is

$$t_{\rm front} \sim 10 \text{ years } \left(\frac{h/r}{0.05}\right)^{-1} \left(\frac{\alpha}{0.3}\right)^{-1} \left(\frac{r}{225 r_g}\right)^{3/2} \frac{r_g}{c} \tag{7}$$

[3] A change to an advection-dominated accretion flow (ADAF) is also fully possible in this model.

which is plausible, if there exists a very viscous disk and the effect propagates outwards on a timescale of ≤ 10 years from the inner disk. This would suppress the UV/X-ray emission from the RIAF (down by a few orders of magnitude from the intensity expected from a thin disk intensity) and explain the broadline behaviour. ADAF spectra are flat in νL_ν Abramowicz & Fragile [2], Abramowicz et al. [3], Narayan et al. [34], and convective ADAFs rise towards X-ray energies. ADAFs exist at lower luminosity, where $\varepsilon \sim 0.005$ for $L = \varepsilon \dot{M} c^2$, lower than the fiducial $\varepsilon \sim 0.1$ for a classic thin disk luminosity.

However, suppressing the flux from the inner disk radii ($\lesssim 225 r_g$) in the low temperature thin disk model [4, 5, 14, 15, 33] by a factor of 20 would still not describe the 2010 spectrum. To restore the thin disk spectrum by 2016, the disk change has to propagate back inwards, most of the way to the ISCO and therefore $t_{\rm front}$ needs to be shorter. This requires h/r to be larger in Equation 7 above, by a factor of ~ 2.

It is unclear what physical processes would trigger the change of state to an ADAF and then cool back down to a thin disk. In any case, suppressing the MCD temperature profile inside a radius of $r_{alt} = 225 r_g$ leads to a collapse in the total flux compared to unperturbed disk. We show some example cases in Figure 1. Clearly, these scenarios are difficult to reconcile with our data.

MODEL 'B': PROPOGATION OF A COOLING FRONT: An alternative model connected to the accretion disk is that a *cooling* front propagates through the thin disk. In order to reproduce the steep fall at $\lambda \leq 200$nm in the 2010 spectrum, a cool phase leads to absorption at short wavelengths.

Initially a modestly fat disk ($h/r \sim 0.2$) with a modest α, cools from the ISCO and propagates outward in a cooling front, collapsing the disk. As the hot disk ($\sim 10^{5-6}$K) cools, it fragments into cooler clumps around $\sim 10^4$K [see e.g., 27]. The main coolants $> 10^{4.5}$K are resonance lines in Carbon and Oxygen and at lower temperatures, H and He from neutral phase material [see e.g., Fig. 18 in 45]. The ionization energies for carbon and oxygen are 11.26 and 13.61 eV, respectively, i.e., ~ 100nm, and hence at wavelengths < 100nm the disk opacity will increase dramatically in an edge. However, the gas in the disk is pressure, turbulence and Doppler broadened, so these ionization edges will manifest around 100nm with decreasing opacity to shorter wavelengths as

$$\kappa \propto \rho T^{-1/2} \nu^{-3} \tag{8}$$

for Kramers' opacities. This implies $\kappa \propto \lambda^3$ at increasing wavelengths up to the ionization edge around 100nm. These features will be blurred (by the broadening) and the ionization edges due to the C and O resonance lines in the cool phase of this disk will be span $50 - 200$nm, depressing the flux at these energies. We note this closely resembles the opacity curve inferred by Guo et al. [16] in J2317+0005 over relevant wavelengths.

The 2010 spectrum in this model comes from a cooler disk plus the increased opacity at short wavelengths in the cooler phase. Heating occurs from the outside in, explaining the 2016 spectrum and asymmetric recovery in photometry. Since the optical continuum has been rising again since mid-2016, this leads to a prediction of a rise in Hydrogen emission line flux in the next few months. The infrared flux returns in 2021.

Acknowledgements

NPR acknowledges support from the STFC and the Ernest Rutherford Fellowship scheme. KESF & BM are supported by NSF PAARE AST-1153335. KESF & BM thank CalTech/JPL for support during sabbatical. MF acknowledges support from NSF grants AST-1518308, AST-1749235, AST-1413600 and NASA grant 16-ADAP16-0232.

This publication makes use of data products from the Wide-field Infrared Survey Explorer, which is a joint project of the University of California, Los Angeles, and the Jet Propulsion Laboratory/California Institute of Technology, and NEOWISE, which is a project of the Jet Propulsion Laboratory/California Institute of Technology. WISE and NEOWISE are funded by the National Aeronautics and Space Administration.

This research has made use of the NASA/IPAC Extragalactic Database (NED) which is operated by the Jet Propulsion Laboratory, California Institute of Technology, under contract with the National Aeronautics and Space Administration.

This research has made use of data obtained from the SuperCOSMOS Science Archive, prepared and hosted by the Wide Field Astronomy Unit, Institute for Astronomy, University of Edinburgh, which is funded by the UK Science and Technology Facilities Council.

The GALEX GR6/7 Data Release hosted at http://galex.stsci.edu/GR6/ was used These data were obtained from the Mikulski Archive for Space Telescopes (MAST). STScI is operated by the Association of Universities for Research in Astronomy, Inc., under NASA contract NAS5-26555. Support for MAST for non-HST data is provided by the NASA Office of Space Science via grant NNX09AF08G and by other grants and contracts.

Funding for SDSS-III has been provided by the Alfred P. Sloan Foundation, the Participating Institutions, the National Science Foundation, and the U.S. Department of Energy Office of Science. The SDSS-III web site is http://www.sdss3.org/. SDSS-III is managed by the Astrophysical Research Consortium for the Participating Institutions of the SDSS-III Collaboration including the University of Arizona, the Brazilian Participation Group, Brookhaven National Laboratory, Carnegie Mellon University, University of Florida, the French Participation Group, the German Participation Group, Harvard University, the Instituto de Astrofisica de Canarias, the Michigan State/Notre Dame/JINA Participation Group, Johns Hopkins University, Lawrence Berkeley National Laboratory, Max Planck Institute for Astrophysics, Max Planck Institute for Extraterrestrial Physics, New Mexico State University, New York University, Ohio State University, Pennsylvania State University, University of Portsmouth, Princeton University, the Spanish Participation Group, University of Tokyo, University of Utah, Vanderbilt University, University of Virginia, University of Washington, and Yale University.

References

[1] Abell G. O., 1959, Leaflet of the Astronomical Society of the Pacific, 8, 121

[2] Abramowicz M. A., Fragile P. C., 2013, Living Reviews in Relativity, 16, 1

[3] Abramowicz M. A., Igumenshchev I. V., Quataert E., Narayan R., 2002, ApJ, 565, 1101

[4] Afshordi N., Paczyński B., 2003, ApJ, 592, 354

[5] Agol E., Krolik J. H., 2000, ApJ, 528, 161

[6] Aihara H., et al., 2017, ArXiv e-prints

[7] Appenzeller I., et al., 1998, ApJS, 117, 319

[8] Bae H.-J., Woo J.-H., 2016, ApJ, 828, 97

[9] Becker R. H., White R. L., Helfand D. J., 1995, ApJ, 450, 559

[10] Boller T., Freyberg M. J., Trümper J., Haberl F., Voges W., Nandra K., 2016, Astron. & Astrophys., 588, A103

[11] Cannon R. D., 1975, Proceedings of the Astronomical Society of Australia, 2, 323

[12] Cannon R. D., 1979, The U.K. 1.2m Schmidt telescope and the southern sky survey

[13] Dawson K., et al., 2013, AJ, 145, 10

[14] Ford K. E. S., et al., 2018, in prep.

[15] Gammie C. F., 1999, ApJ Lett., 522, L57

[16] Guo H., et al., 2016, ApJ, 826, 186

[17] Hambly N. C., et al., 2001, MNRAS, 326, 1279

[18] Hambly N. C., Irwin M. J., MacGillivray H. T., 2001, MNRAS, 326, 1295

[19] Hopkins P. F., 2013, MNRAS, 428, 2840

[20] Kepler S. O., et al., 2015, MNRAS, 446, 4078

[21] Kepler S. O., et al., 2016, MNRAS, 455, 3413

[22] King A. R., Pringle J. E., Livio M., 2007, MNRAS, 376, 1740

[23] Lang D., 2014, AJ, 147, 108

[24] Mainzer A., et al., 2011, ApJ, 731, 53

[25] Margala D., Kirkby D., Dawson K., Bailey S., Blanton M., Schneider D. P., 2016, ApJ, 831, 157

[26] Martin D. C., et al., 2005, ApJ Lett., 619, L1

[27] McCourt M., Oh S. P., O'Leary R. M., Madigan A.-M., 2016, ArXiv e-prints

[28] Meisner A. M., Bromley B. C., Nugent P. E., Schlegel D. J., Kenyon S. J., Schlafly E. F., Dawson K. S., 2017, AJ, 153, 65

[29] Meisner A. M., Lang D., Schlegel D. J., 2017, AJ, 154, 161

[30] Minkowski R. L., Abell G. O., 1963, The National Geographic Society-Palomar Observatory Sky Survey. the University of Chicago Press, p. 481

[31] Morrissey P., et al., 2007, ApJS, 173, 682

[32] Nagakura H., Yamada S., 2008, ApJ, 689, 391

[33] Narayan R., Kato S., Honma F., 1997, ApJ, 476, 49

[34] Narayan R., Mahadevan R., Quataert E., 1998, in Abramowicz M. A., Björnsson G., Pringle J. E., eds, Theory of Black Hole Accretion Disks Advection-dominated accretion around black holes. pp 148–182

[35] Nemmen R. S., Storchi-Bergmann T., Yuan F., Eracleous M., Terashima Y., Wilson A. S., 2006, ApJ, 643, 652

[36] Quataert E., 2001, in Peterson B. M., Pogge R. W., Polidan R. S., eds, Probing the Physics of Active Galactic Nuclei Vol. 224 of Astronomical Society of the Pacific Conference Series, Low Radiative-Efficiency Accretion Flows. p. 71

[37] Richards G. T., et al., 2002, AJ, 123, 2945

[38] Ross N. P., et al., 2012, ApJS, 199, 3

[39] Schneider D. P., et al., 2002, AJ, 123, 567

[40] Shakura N. I., Sunyaev R. A., 1973, Astron. & Astrophys., 24, 337

[41] Shen Y., et al., 2011, ApJS, 194, 45

[42] Shiokawa H., Krolik J. H., Cheng R. M., Piran T., Noble S. C., 2015, ApJ, 804, 85

[43] Stern D., et al., 2018, ApJ

[44] Stoughton C., et al., 2002, AJ, 123, 485

[45] Sutherland R. S., Dopita M. A., 1993, ApJS, 88, 253

[46] Voges W., et al., 1999, Astron. & Astrophys., 349, 389

[47] Wright E. L., et al., 2010, AJ, 140, 1868

[48] Yuan F., Narayan R., 2014, ARA&A, 52, 529

[49] Zimmerman E. R., Narayan R., McClintock J. E., Miller J. M., 2005, ApJ, 618, 832